Direct-photon pair production

C. Carimalo, M. Crozon, P. Kessler, and J. Parisi
Laboratoire de Physique Corpusculaire, Collège de France, Paris, France
(Received 29 June 1983; revised manuscript received 13 February 1984)

Direct-photon pair production in high-energy hadron collisions is considered. After discussing general aspects of such reactions and giving a brief historical survey of the subject, we present some calculations on the contributions from $q\bar{q}$ and gg collisions (the latter via the quark box) to the $\gamma\gamma$ continuum, and on possible resonant contributions. Finally, an estimation of the indirect-photon background (mainly due to π^0 and η decay, and to quark bremsstrahlung) is given for colliding-beam conditions at high energy; assuming both photons to be measured at 90° with equal and opposite momenta, and (within experimental limits) unaccompanied by any hadrons or additional photons, it is shown that this background can be sharply reduced.

I. INTRODUCTION

A. General aspects

Direct-photon pair production in hadron collisions is quite similar, in many respects, to lepton pair production, which has been extensively studied by high-energy physicists for many years. Both processes should provide, in the first place, a check of the quark model, since the primary mechanism involved—provided the photons or leptons are emitted at sufficiently high transverse momentum—should in both cases be that of a quark-antiquark collision [Figs. 1(a) and 1(b)]. One however notices that, compared to l^+l^- production (Drell-Yan process[1]), photon pair production has the additional property of allowing one to check the quark propagator. Another difference is that whereas in Fig. 1(b) the squares of the quark charges are involved, it is the fourth power of those charges that enters the computation of the graph of Fig. 1(a).

Higher-order QCD corrections to be computed for Fig. 1(a) (see Sec. II) are partly similar and partly different, as compared to those pertaining to Fig. 1(b). In particular, the Feynman graph of Fig. 2 is specific to photon pair production; as we shall see, its contribution may become important, even predominant, under certain conditions. Thus the type of process considered here may also become an excellent tool for checking higher-order quantum chromodynamics.

On the other hand, it should be possible to use both photon pair and lepton pair production for investigating the existence of new resonant structures, as shall be discussed (for photon pairs) in Sec. III. As regards l^+l^- production, one notices that it was through that kind of process that the J/ψ and the Υ were discovered.[2,3] Whereas resonances decaying into lepton pairs are expected to have the quantum numbers of the photon ($J=1$, $P=-1$, $C=-1$), two-photon final states may proceed, according to Yang's selection rules,[4] from a much larger variety of resonant structures, involving quantum numbers $0^{++},0^{-+},2^{++},2^{-+},3^{++},\ldots$. Those structures may either belong to known quarkonium families (as would be the case for the η_b, for instance) or be new ones (such as massive gluonia, or possible quarkonium states made of scalar-quark pairs).

Lepton pair and photon pair production have still something else in common. Both are the reverse processes of well-known and widely studied types of reactions: e^+e^- annihilation and $\gamma\gamma$ collisions, respectively, both of which are produced in electron-positron storage rings or colliders. Insofar as a given process and the reverse one may be considered as competing with each other for the investigation of a particular phenomenon (search for a new resonant structure, for instance), one should notice the following: While, generally speaking, lepton pair production is a much more complicated process than e^+e^- annihilation, the mechanisms involved in photon pair pro-

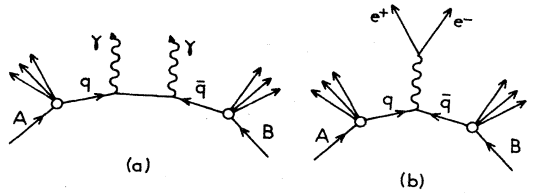

FIG. 1. Feynman diagrams for (a) photon pair and (b) lepton pair production through quark-antiquark collisions.

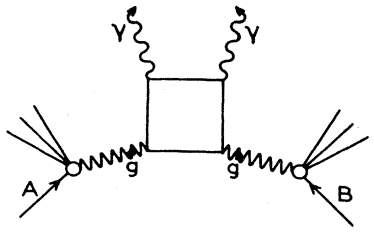

FIG. 2. Feynman diagram for photon pair production through gluon-gluon scattering via a quark box (additional contributing diagrams are obtained by permuting the external legs).

duction are, in principle, of no greater complexity than the $\gamma\gamma$ collision mechanism with electron-positron colliding beams.

We conclude that, from various points of view, photon pair production is at least as interesting a process as lepton pair production. The reason why the former is still much less popular than the latter is an obvious experimental one: While event rates should be about the same for both types of reactions (as we shall see), background problems appear to be much more complex in photon pair production, due to the occurrence of indirect photons proceeding in particular from π^0's and other neutral mesons. From a recent measurement performed at the CERN ISR[5] it appears however that those background problems can, at least to some extent, be kept under control. On the other hand, in Sec. IV, we shall make a detailed discussion and an estimation of the indirect-photon background in photon pair production for colliding-beam conditions at high energy.

B. History

Whereas there exists a vast theoretical and experimental literature on lepton pair production, direct-photon pair production has been studied until now by a small number of authors. In their fundamental paper of 1971 on hard-collision processes, Berman, Bjorken, and Kogut[6] mentioned $q\bar{q}\to\gamma\gamma$ as one of the elementary reactions to be considered. Many years later (from 1978 on), some authors started studying various applications of that elementary process. Soh, Pac, Lee, and Choi[7] suggested that it might be possible to derive the ratio α_s/α from an experimental comparison between γg and $\gamma\gamma$ production in hadron collisions. Krawczyk and Ochs,[8] considering $\gamma\gamma$ as well as e^+e^- and $\pi^0\pi^0$ production in $\pi^\pm p$ collisions, provided several interesting predictions, in particular, regarding the differences between yields obtained in π^+p and π^-p collisions. Hemmi[9] suggested that a hint might be obtained on the quark mass (via the quark-propagator effect) by measuring the production cross section and the photons' angular distribution in $AB\to\gamma\gamma X$. Combridge[10] and, independently, the authors of this paper,[11] studied the contribution of the subprocess $gg\to\gamma\gamma$, involving the quark-box diagram (Fig. 2) to direct-photon pair production. Contogouris, Marleau, and Pire[12] studied the ratio of $\gamma\gamma$ to $\pi^0\pi^0$ production at high p_T in pp collisions. In the first experiment on direct-photon pair production, recently performed by Kourkoumelis *et al.*,[5] the reaction $pp\to\gamma\gamma X$ was studied at $\sqrt{s}=63$ GeV; the ratio $\gamma\gamma/e^+e^-$ was found to be in rough agreement with theoretical predictions. Most recently, Field provided a survey on large-p_T single- and double-photon production in pp, $\bar{p}p$, and $\pi^\pm p$ collisions.[13]

II. CONTINUUM CONTRIBUTION

A. Contributions of $q\bar{q}\to\gamma\gamma$

Considering the type of process represented in Figs. 1(a) and 1(b), with a pair of particles (photons or leptons) measured at large, equal, and opposite transverse momentum p_T, we shall use the general notation

$$\bar{\sigma}\equiv\left[\frac{d\sigma}{dp_T d\theta\, d\theta'}\right]_{\theta=\theta'=90^\circ},$$

where θ,θ' are the emission angles of both particles measured in the overall c.m. frame (or, as well, in their own c.m. frame).

Ignoring intrinsic parton momenta and QCD higher-order corrections, one gets[14] for the process described by Fig. 1(a)

$$\bar{\sigma}_{(q\bar{q})}^{AB\to\gamma\gamma X}=\frac{2x}{\sqrt{s}}\sum_{q=u,d,s}[q_A(x)\bar{q}_B(x)+\bar{q}_A(x)q_B(x)]\times\tilde{\sigma}^{q\bar{q}\to\gamma\gamma}, \tag{2.1}$$

where $x=2p_T/\sqrt{s}$, s being the total c.m. energy squared; q_A (q_B) is the distribution function defining the quark content of particle A (B); $\bar{q}_A$ ($\bar{q}_B$) are the analogous functions for antiquarks; $\tilde{\sigma}$ is defined for a two-body reaction as

$$\tilde{\sigma}\equiv\left[\frac{d\sigma}{d(\cos\theta)}\right]_{\theta=90^\circ}.$$

For the process considered here one gets (taking account of charge and color)

$$\tilde{\sigma}^{q\bar{q}\to\gamma\gamma}=\frac{\pi\alpha^2 e_q{}^4}{12p_T{}^2}, \tag{2.2}$$

where e_q is the charge of a given quark.

For comparison, we now consider the Drell-Yan process, as shown in Fig. 1(b). In analogy with (2.1), one gets

$$\bar{\sigma}_{(q\bar{q})}^{AB\to l^+l^-X}=\frac{2x}{\sqrt{s}}\sum_{q=u,d,s}[q_A(x)\bar{q}_B(x)+\bar{q}_A(x)q_B(x)]\tilde{\sigma}^{q\bar{q}\to l^+l^-}, \tag{2.3}$$

where

$$\tilde{\sigma}^{q\bar{q}\to l^+l^-}=\frac{\pi\alpha^2 e_q{}^2}{24p_T{}^2}. \tag{2.4}$$

One gets the ratio

$$R\equiv\frac{\bar{\sigma}_{(q\bar{q})}^{AB\to\gamma\gamma X}}{\bar{\sigma}_{(q\bar{q})}^{AB\to l^+l^-X}}=2\frac{\sum_{q=u,d,s}e_q{}^4[q_A(x)\bar{q}_B(x)+\bar{q}_A(x)q_B(x)]}{\sum_{q=u,d,s}e_q{}^2[q_A(x)\bar{q}_B(x)+\bar{q}_A(x)q_B(x)]}. \tag{2.5}$$

It is easily seen that this ratio must lie, in any case, between $\frac{2}{9}$ and $\frac{8}{9}$. More precisely, according to the most usual models for quark distribution functions ($\bar{u}=\bar{d}=\bar{s}=s$ for the proton and $\bar{u}=d=\bar{s}=s$ for π^+), as one goes from the range where sea quarks dominate ($x\ll 0.1$) to that dominated by valence quarks ($x\gg 0.1$), R varies from $\frac{2}{3}$ to $\frac{8}{9}$ in pp, $p\bar{p}$, π^-p, and π^-n collisions; from $\frac{2}{3}$ to $\frac{34}{45}$ in pn and $\bar{p}n$ collisions; and from $\frac{2}{3}$ to $\frac{2}{9}$ in

π^+p and π^+n collisions. In conclusion, $\gamma\gamma$ production due to the $q\bar{q}$ mechanism should always be slightly inferior to Drell-Yan l^+l^- production (at the same values of s and p_T, in the configuration considered).

First-order QCD corrections, as shown in Fig. 3, have not yet been computed. However Contogouris, Marleau, and Pire[12] have shown that, in the soft-gluon approximation, a correction factor given by

$$1+(\alpha_s/2\pi)C_F\pi^2 ,$$

with $C_F=\frac{4}{3}$ in color SU(3), should be applied to the result of the zeroth-order calculation. Such a correction, which according to those authors happens to be the same as for the Drell-Yan process, amounts (with $\alpha_s\simeq 0.25$) to an enhancement of about 50%.

B. Contribution of $gg\to\gamma\gamma$

Considering the Feynman graph of Fig. 2 and factorizing as in Sec. II A, one obtains

$$\bar{\sigma}_{(gg)}^{AB\to\gamma\gamma X}=\frac{2x}{\sqrt{s}}g_A(x)g_B(x)\tilde{\sigma}^{gg\to\gamma\gamma} , \tag{2.6}$$

where g_A (g_B) is the distribution function describing the gluon content of particle A (B), and where one obtains for $\tilde{\sigma}^{gg\to\gamma\gamma}$ the expression[15]

$$\tilde{\sigma}^{gg\to\gamma\gamma}=\frac{25}{2592}\frac{\pi\alpha^2\alpha_s{}^2}{p_T{}^2} \tag{2.7}$$

which takes account of color and of charge factors (the quark box is assumed to involve u, d, s, and c quarks).

If we compare $\gamma\gamma$ production through the gg and the $q\bar{q}$ mechanisms, respectively, we get

$$R'\equiv\frac{\bar{\sigma}_{(gg)}^{AB\to\gamma\gamma X}}{\bar{\sigma}_{(q\bar{q})}^{AB\to\gamma\gamma X}}=\frac{25}{216}\alpha_s{}^2\frac{g_A(x)g_B(x)}{\sum_{q=u,d,s}e_q{}^4[q_A(x)\bar{q}_B(x)+\bar{q}_A(x)q_B(x)]} . \tag{2.8}$$

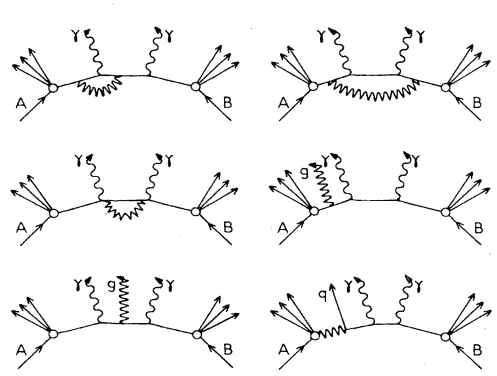

FIG. 3. Feynman diagrams for computing first-order QCD corrections to the basic diagram of Fig. 1 (additional contributing diagrams are obtained by left-right symmetry).

It is then seen that, in the range of very small x values—where the gluon content of a hadron should be considerably larger than its quark or antiquark content—the ratio R' might become of the order of 1 or even larger. This somewhat surprising fact has already been emphasized in Refs. 10 and 11.

Again according to Contogouris, Marleau, and Pire,[12] the first-order QCD correction to the graph of Fig. 2, as computed in the soft-gluon approximation, gives rise to a correction factor of

$$1+(\alpha_s/2\pi)N_c\pi^2$$

with $N_c=3$ in color SU(3); i.e. (with $\alpha_s\simeq 0.25$) to an enhancement of about 110%.

III. RESONANT CONTRIBUTIONS

Since most resonant structures coupled to two photons in accordance with Yang's selection rules[4] may be expected as well to be coupled to two gluons,[16] it seems quite obvious to assume that their production mechanism in hadron collisions should be that of the "gluon fusion model" of Einhorn and Ellis,[17] as shown in Fig. 4. Using again factorization, one here obtains

$$\bar{\sigma}_{(R)}^{AB\to\gamma\gamma X}=\frac{2x}{\sqrt{s}}g_A(x)g_B(x)\tilde{\sigma}^{gg\to R\to\gamma\gamma} , \tag{3.1}$$

where (in a narrow-resonance approximation, i.e., for $\Gamma_R\ll M_R$, calling Γ_R and M_R the total width and the mass, respectively, of the resonance) the last factor is given by

$$\tilde{\sigma}^{gg\to R\to\gamma\gamma}\simeq\frac{\pi^2(2J_R+1)}{64p_T{}^2}\frac{\Gamma(R\to gg)\Gamma(R\to\gamma\gamma)}{\Gamma_R}\times\delta(M_R-2p_T)[f_R(\theta)]_{\theta=90^\circ} , \tag{3.2}$$

where J_R is the resonance's spin, and the angular-distribution function $f_R(\theta)$ is normalized in such a way that

$$\int_0^\pi f_R(\theta)\sin\theta\,d\theta=1 ;$$

e.g., when $J_R=0$, $f_R(\theta)=\frac{1}{2}$.

It seems reasonable to assume that, in most cases, the two-gluon channel would be the main decay channel of

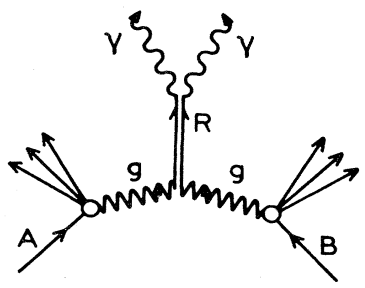

FIG. 4. Feynman diagram for photon pair production through gluon-gluon scattering via a resonance.

the resonance considered, so that we may take $\Gamma(R\to gg)\approx\Gamma_R$. Then one gets

$$\bar{\sigma}^{gg\to R\to\gamma\gamma}\simeq\frac{\pi^2(2J_R+1)}{64{p_T}^2}\times\Gamma(R\to\gamma\gamma)\delta(M_R-2p_T)[f_R(\theta)]_{\theta=90^\circ}\,. \tag{3.3}$$

Now it appears obvious that, if such resonant structures ever show up in $\gamma\gamma$ production, it will be in the small-x range where the gluon content of hadrons should be high. On the other hand we have seen in Sec. II B that, when x becomes small enough, the $\gamma\gamma$ continuum might become dominated by the gg contribution. It thus seems interesting to compare (3.1) with (2.6), i.e., in fact (3.3) with (2.7). One gets the ratio

$$R''\equiv\frac{\bar{\sigma}_{(R)}^{AB\to\gamma\gamma X}}{\bar{\sigma}_{(gg)}^{AB\to\gamma\gamma X}}=\frac{81\pi(2J_R+1)\Gamma(R\to\gamma\gamma)}{50\alpha^2{\alpha_s}^2}\delta(M_R-2p_T)[f_R(\theta)]_{\theta=90^\circ}\,. \tag{3.4}$$

Using a conventional procedure, we shall replace $\delta(M_R-2p_T)$ by $(2\Delta p_T)^{-1}$, calling Δp_T the experimental momentum resolution of either photon (we assume here colliding-beam conditions, i.e., the laboratory frame is the overall c.m. frame). Then

$$R''=\frac{81\pi(2J_R+1)\Gamma(R\to\gamma\gamma)}{100\alpha^2{\alpha_s}^2\Delta p_T}[f_R(\theta)]_{\theta=90^\circ}\,. \tag{3.5}$$

If now we make the following assumptions regarding the various parameters involved, (i) $J_R=0$, thus $f_R(\theta)=\frac{1}{2}$, (ii) $\Gamma(R\to\gamma\gamma)=1$ keV, (iii) Δp_T (GeV)$=0.1$ $[p_T$ (GeV)$]^{1/2}$, and in addition (iv) $\alpha_s=0.25$, (v) $M_R=10$ GeV, thus $\Delta p_T\simeq0.22$ GeV, we get $R''\simeq1.5$.

We therefore conclude that, keeping x sufficiently small, there is some hope of seeing at least some resonant structures coupled to two photons, as they might show up above the nonresonant background.

That conclusion is confirmed by the curve shown in Figs. 5 and 6, where it has been assumed that a resonant structure might occur at any value of $M_R=2p_T$, and where the corresponding $\bar{\sigma}$ value has been computed according to the above-made assumptions (i)—(iii). Under those assumptions, it appears, in particular, that in $p\bar{p}$ collisions at $\sqrt{s}=540$ GeV, a resonant contribution would remain larger than the total contribution of the $\gamma\gamma$ continuum (due to the $q\bar{q}$ plus the gg mechanism) up to $M_R\simeq12$ GeV.

Figures 5 and 6 also confirm that $\gamma\gamma$ production due to the $q\bar{q}$ mechanism always remains slightly smaller than l^+l^- production through the Drell-Yan process; and that

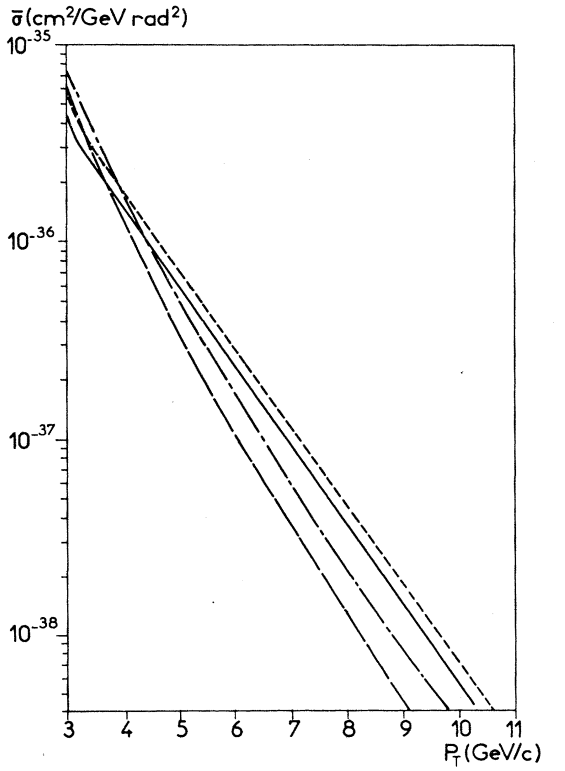

FIG. 5. Various contributions to $\bar{\sigma}^{pp\to\gamma\gamma X}$ at $\sqrt{s}=60$ GeV. Solid curves, $q\bar{q}$ contribution; long-dashed curve, gg contribution; dot-dash curve, contribution of a hypothetical resonant structure of arbitrary mass (we let that mass, $M_R=2p_T$, vary continuously). For comparison, $\bar{\sigma}^{pp\to l^+l^-}$ is also shown (short-dashed) curve.

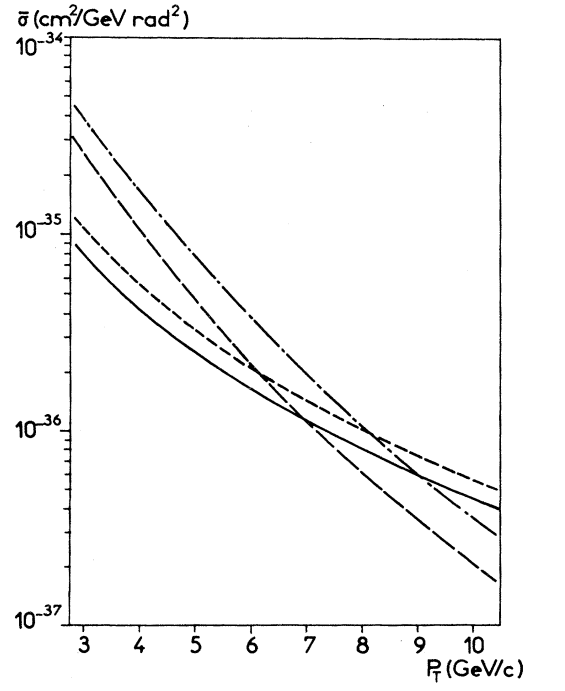

FIG. 6. Same as Fig. 5, for $\bar{\sigma}^{p\bar{p}\to\gamma\gamma X}$ at $\sqrt{s}=540$ GeV.

the gg mechanism dominates over the $q\bar{q}$ mechanism in some small-x range, i.e., up to $p_T \simeq 3.5$ GeV in pp collisions at $\sqrt{s}=60$ GeV, and up to $p_T \simeq 7$ GeV in $p\bar{p}$ collisions at 540 GeV.

For the various distribution functions we here used the scale-violating parametrization of Baier, Engels, and Petersson,[18] with the following ingredients: $Q^2=\frac{4}{3}p_T^2$; $Q_0^2=5$ GeV^2; $\Lambda=0.3$ GeV. In the expression for the running coupling constant,

$$\alpha_s = 12\pi/(25\ln Q^2/\Lambda^2) ,$$

the same definition of Q^2 and the same value of Λ were used. We are of course aware that, as emphasized by Field,[13] predictions provided by any model for very small-x values (such as occur in Fig. 6) should be considered as rough ones.

Let us finally remark that, given the decrease with p_T of the yields computed, and considering the luminosities of the colliding-beam devices concerned (ISR, CERN collider), it would not make much sense to extend our predictions (in both Figs. 5 and 6) beyond $p_T \simeq 10$ GeV.

IV. A BACKGROUND STUDY FOR $\gamma\gamma$ PRODUCTION AT COLLIDER ENERGIES

In this section a quantitative study will be made of the contamination of direct $\gamma\gamma$ production by indirect photons proceeding from various sources, under the same conditions as considered in Secs. II and III. After discussing indirect-photon sources and defining an appropriate formalism for computing the corresponding contamination, we shall give numerical predictions for the noise/signal ratio under the additional assumption that (within certain experimental limits) both photons measured are unaccompanied by any hadrons or additional photons. Among the mechanisms involved in that background computation, we shall consider, in addition to jet production and fragmentation, a possible contribution from the Brodsky-Lepage mechanism where particle pairs are directly created in a hard collision.

A. Indirect-photon sources

1. Neutral pions

It is well known that the main source of indirect photons are neutral pions, since the latter decay into two photons with a branching ratio of 99%, and since those two decay photons may be mistaken for a single one in various configurations, which are the following.

(i) In the configuration schematically represented in Fig. 7(i) a neutral pion decays so unsymmetrically that the energy of one of the photons becomes too small to allow it to be detected. A calculation (simply based on kinematics and on the fact that the angular distribution of the decay photons is isotropic in the π^0's rest frame) shows that the proportion of neutral pions decaying in such a way that one decay photon has its energy lower than some limit $\Delta E^{(\gamma)}$ is $2\Delta E^{(\gamma)}/E_\pi$. A reasonable experimental value for that limit should be $\Delta E^{(\gamma)} \simeq 200$–$300$ MeV.

(ii) Another configuration to be considered [Fig. 7(ii)] is the one where the angle between the decay photons is so large that one of them falls within the acceptance of the apparatus, while the other one does not. Actually the kinematics of the two-body decay is such that a large angular separation between the photons corresponds to a large difference in their energies. Therefore configuration (ii) overlaps with (i), i.e., its contribution to the indirect-photon background is already partly taken into account by considering (i). The rest of that contribution can be suppressed by dividing the experimental acceptance into a restricted fiducial volume plus an adjacent angular range where any additional photon would be vetoed. The extension of that angular range should be given by

$$\Delta\theta \simeq m_\pi/(E_\gamma \Delta E^{(\gamma)})^{1/2} ,$$

where E_γ is the energy of the photon measured; typically, for $E_\gamma=5$ GeV and $\Delta E^{(\gamma)}=250$ MeV, one gets $\Delta\theta \simeq 7°$.

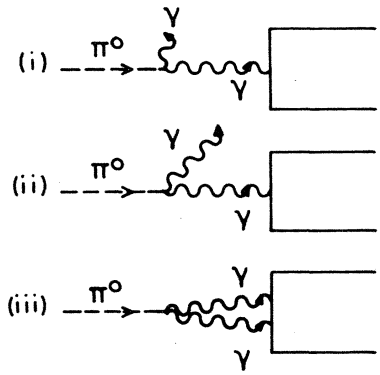

FIG. 7. Various experimental configurations where a π^0 may be mistaken for a photon. (i) One of the decay photons has very little energy. (ii) The angular separation between the photons is so large that only one of them falls into the acceptance of the apparatus. (iii) The angular separation is so small that the photons "merge."

(iii) Finally the third dangerous configuration is that of Fig. 7(iii), where the angle between the decay photons becomes so small that they "merge," i.e., they are seen as a single photon whose apparent energy is the full energy of the pion. Using elementary kinematics here again, it is seen that the minimal angular separation between the two photons is $2m_\pi/E_\pi$. Since experimentalists would admit that it is possible to achieve an angular resolution of 25–30 mrad or so, that phenomenon of nonseparability should be avoidable as long as one looks for photons with an energy of less than about 10 GeV.

In conclusion we shall take account only of configuration (i).

2. Other mesons

After the neutral pion, the most important source of indirect photons, among the other mesons, is provided by the η which decays into two photons with a branching ratio of 39%. The problems occurring with the η are the same as discussed above for the π^0, apart from the following quantitative differences due to the change in mass ($m_\eta \simeq 4m_\pi$). As regards configuration (ii), the angular veto range needed for its suppression should be about four times larger than that required in the π^0 case, e.g., for

$E_\gamma = 5$ GeV and $\Delta E^{(\gamma)} = 250$ MeV one should have $\Delta\theta \simeq 30°$ (we may assume that under colliding-beam collisions, the outgoing photons being measured at about 90°, it should be possible to use such a wide veto range); on the other hand the risk of "merger" of the decay photons [configuration (iii)] here only occurs (again assuming an angular resolution of 25–30 mrad) at $E_\gamma \gtrsim 40$ GeV. If finally one here again retains only configuration (i) as providing an unavoidable background in a direct-photon measurement, it results—similar to what was found above for neutral pions—that the proportion of η's contributing to that background is $2\Delta E^{(\gamma)}/E_\eta$.

Account should also be taken of indirect-photon production by the η', decaying into $\gamma\gamma$ with a branching ratio of 2% and into $\rho^0\gamma$ with a branching ratio of 30%; and by the ω, decaying into $\pi^0\gamma$ with a branching ratio of 9%. One notices that the η' and the ω, as well as the η, tend to be slightly less abundantly produced in hadron-hadron collisions than the neutral pion.[19]

Forgetting about the relatively unimportant modes $\eta' \to \gamma\gamma$, $\omega \to \pi^0\gamma$, we shall also neglect the contribution of the mode $\eta' \to \rho^0\gamma$, for the following reason: elementary kinematics show that the minimal energy of the ρ^0 should be

$$E_\rho^{\min} \simeq (m_\rho{}^2/m_{\eta'}{}^2) E_{\eta'} \simeq \tfrac{2}{3} E_{\eta'} ,$$

since we shall assume further below that an upper limit $\Delta E^{(h)}$ of at most a few GeV can be experimentally imposed to the total energy of the hadrons accompanying either photon measured, that background will be entirely excluded.

In conclusion, we will only take account of the neutral pion and the η as mesonic sources of indirect photons. For simplicity we shall assume, in addition, that the number of η's produced in the hadronic collisions considered is equal to that of π^0's. That assumption involves some overestimation which should compensate, more or less, for our neglect of the other mesons' contribution.

3. *Quarks and gluons*

In our background calculations we shall include the contribution from quarks and gluons radiating (or, equivalently, fragmenting into) photons via QCD. We are aware that other authors[12,13] would consider such radiative processes as contributing to the signal rather than to the background. We however feel that those rather indirect modes of photon pair production are of little physical interest (like most bremsstrahlung processes) and therefore should indeed be treated as parasite effects.

B. Formalism for background calculations

Assuming an experiment where one will measure two photons emitted at 90° with equal and opposite momenta, we are led to consider, in the most general way, two types of indirect-photon background.

(i) Background due to reactions $AB \to c\gamma X$ followed by $c \to \gamma + \ldots$, where c is either a parton (quark or gluon) or a particle (a meson); c is assumed, in first approximation, to be emitted as well at 90°, and its momentum is defined by p_T/z (with $2p_T/\sqrt{s} \le z \le 1$).

(ii) Background due to reactions $AB \to cdX$ followed by $c \to \gamma + \ldots, d \to \gamma + \ldots$, where c,d are again partons or particles, assumed to be emitted at 90°, in first approximation, their momenta being given, respectively, by $p_T/z, p_T/z'$ (with $2p_T/\sqrt{s} \le z,z' \le 1$).

In both cases the initial reaction is assumed to involve a hard collision, i.e., $ab \to c\gamma$ in case (i), $ab \to cd$ in case (ii). If we neglect, as before (Secs. II and III), the intrinsic transverse momentum of the initial partons a,b, we notice that background (i) is entirely suppressed because of the correlation $z=1$, while we also get a very stringent correlation, $z=z'$, for background (ii). This is obviously not realistic, and therefore we will introduce an intrinsic transverse momentum $\vec{k}_T$ for either initial parton. We then obtain, generalizing a treatment given by Gunion and Petersson,[20] and summing over both types of reactions (i) and (ii):

$$\sum_{a,b,c} \frac{d\sigma_{(ab)}^{AB\to c\gamma X\to\gamma\gamma X'}}{(d^3p_\gamma/E_\gamma)(d^3p'_\gamma/E'_\gamma)} + \sum_{a,b,c,d} \frac{d\sigma_{(ab)}^{AB\to cdX\to\gamma\gamma X'}}{(d^3p_\gamma/E_\gamma)(d^3p'_\gamma/E'_\gamma)}$$
$$= \frac{1}{\pi^2 s\langle k_T{}^2\rangle} \int \frac{dz}{z^2}\frac{dz'}{z'^2} F(z,z') \sum_{a,b} a_A^{(z,z')} b_B^{(z,z')} \left[\sum_c \tilde{\sigma}_{(z,z')}^{ab\to c\gamma} D_{\gamma/c}(z)\delta(z'-1) + \sum_{c,d} \tilde{\sigma}_{(z,z')}^{ab\to cd} D_{\gamma/c}(z) D_{\gamma/d}(z') \right] , \quad (4.1)$$

where

$$F(z,z') = \frac{z+z'}{2\sqrt{zz'}} \exp\left[-\frac{(z-z')^2 p_T{}^2}{2z^2 z'^2 \langle k_T{}^2\rangle} \right] ,$$

a_A and b_B are, respectively, the distribution functions of a in A and b in B; the superscript (z,z') means that they are defined as functions of $x/\sqrt{zz'}$ instead of x, and (in case of scale violation) of Q^2/zz' instead of Q^2. Similarly the subscript (z,z') of $\tilde{\sigma}$ means that the latter becomes a function of $p_T{}^2/zz'$ instead of $p_T{}^2$. Finally, $D_{\gamma/c}(z)$ and $D_{\gamma/d}(z')$ define the probability of obtaining a photon of momentum p_T, either through direct fragmentation or decay or through some cascade process, from a parton or particle c of momentum p_T/z and from a parton or particle d of momentum p_T/z', respectively.

The noise/signal ratio thus becomes

$$r \equiv \frac{\sum_{a,b,c} \frac{d\sigma_{(ab)}^{AB\to c\gamma X\to\gamma\gamma X'}}{(d^3p_\gamma/E_\gamma)(d^3p'_\gamma/E'_\gamma)} + \sum_{a,b,c,d} \frac{d\sigma_{(ab)}^{AB\to cdX\to\gamma\gamma X'}}{(d^3p_\gamma/E_\gamma)(d^3p'_\gamma/E'_\gamma)}}{\sum_{a,b} \frac{d\sigma_{(ab)}^{AB\to\gamma\gamma X}}{(d^3p_\gamma/E_\gamma)(d^3p'_\gamma/E'_\gamma)}}$$

$$= \left[\sum_{a,b} \tilde{\sigma}_{(ab)}^{AB\to\gamma\gamma X}\right]^{-1} \frac{2x}{\sqrt{s}} \int \frac{dz}{z^2}\frac{dz'}{z'^2} F(z,z') \sum_{a,b} a_A^{(z,z')} b_B^{(z,z')} \left[\sum_c \tilde{\sigma}_{(z,z')}^{ab\to c\gamma} D_{\gamma/c}(z)\delta(1-z') + \sum_{c,d} \tilde{\sigma}_{(z,z')}^{ab\to cd} D_{\gamma/c}(z) D_{\gamma/d}(z')\right] . \tag{4.2}$$

In Secs. IV C and IV D we shall compute, using formula (4.2), the contamination due to jet production and fragmentation on one hand, and the more hypothetical one due to the Brodsky-Lepage mechanism on the other hand.

C. Contamination through jet production and fragmentation

Taking account of the background provided by all two-body parton reactions $ab\to c\gamma$ and $ab\to cd$ (Fig. 8), formula (4.2) becomes

$$\begin{aligned} r = (\bar{\sigma}_{(q\bar{q})}^{AB\to\gamma\gamma X} + \bar{\sigma}_{(gg)}^{AB\to\gamma\gamma X})^{-1} \frac{2x}{\sqrt{s}} \int_{z_{\min}}^1 \frac{dz}{z} \int_{z'_{\min}}^1 \frac{dz'}{z'} F(z,z') \\ \times \Bigg\{ \sum_q [(q_A+\bar{q}_A)g_B + g_A(q_B+\bar{q}_B)]\tilde{\sigma}^{qg\to q\gamma} D_q(z)\delta(z'-1) \\ + \left[\sum_q (q_A\bar{q}_B+\bar{q}_Aq_B)\tilde{\sigma}^{q\bar{q}\to g\gamma} + g_Ag_B\tilde{\sigma}^{gg\to g\gamma}\right] D_g(z)\delta(z'-1) \\ + \left[\sum_q (q_A\bar{q}_B+\bar{q}_Aq_B)\tilde{\sigma}^{q\bar{q}\to q\bar{q}} + (q_Aq_B+\bar{q}_A\bar{q}_B)\tilde{\sigma}^{qq\to qq}\right] D_q(z)D_q(z') \\ + \sum_q \sum_{q'\neq q} (q_Aq'_B + q_A\bar{q}'_B + \bar{q}_Aq'_B + \bar{q}_A\bar{q}'_B)\tilde{\sigma}^{qq'\to qq'} D_q(z)D_{q'}(z') \\ + \sum_q \left[\sum_{q'\neq q} (q'_A\bar{q}'_B + \bar{q}'_Aq'_B)\tilde{\sigma}^{q'\bar{q}'\to q\bar{q}} + g_Ag_B\tilde{\sigma}^{gg\to q\bar{q}}\right] D_q(z)D_q(z') \\ + \sum_q [(q_A+\bar{q}_A)g_B + g_A(q_B+\bar{q}_B)]\tilde{\sigma}^{qg\to qg} D_q(z)D_g(z') \\ + \left[\sum_q (q_A\bar{q}_B+\bar{q}_Aq_B)\tilde{\sigma}^{q\bar{q}\to gg} + g_Ag_B\tilde{\sigma}^{gg\to gg}\right] D_g(z)D_g(z') \Bigg\} . \end{aligned} \tag{4.3}$$

Here the sums over q and q' include u,d,s flavors. For simplicity of notation, we have written $q_A,\bar{q}_B$, etc., for $q_A^{(z,z')},\bar{q}_B^{(z,z')}$, etc. On the other hand, the (z,z') dependence has been extracted from the $\tilde{\sigma}$'s (it is simply given by a factor zz'); those differential cross sections are found, for the various reactions $ab\to c\gamma$ considered, to be given (with charge and color factors included) by

$$\tilde{\sigma}^{qg\to q\gamma} = \tilde{\sigma}^{\bar{q}g\to\bar{q}\gamma} = \frac{5\pi\alpha_s\alpha e_q^2}{48p_T^2} , \tag{4.4}$$

$$\tilde{\sigma}^{q\bar{q}\to g\gamma} = \frac{2\pi\alpha_s\alpha e_q^2}{9p_T^2} , \tag{4.5}$$

$$\tilde{\sigma}^{gg\to\gamma\gamma} = \frac{5\pi\alpha_s^3\alpha e_q^2}{1728p_T^2} , \tag{4.6}$$

while, for all reactions $ab\to cd$ considered, they can be taken from Ref. 21.

As for the functions $D_c(z)$ [or the similar ones $D_d(z)$; $c,d\equiv q$ or g], they can be shown, after some kinematic manipulations, to be given by

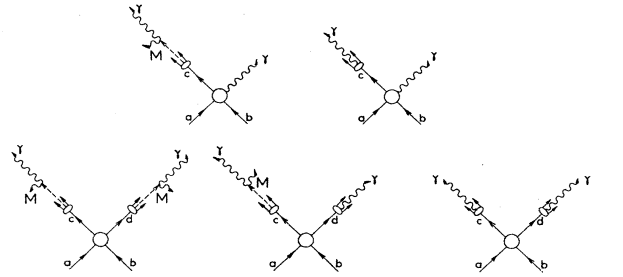

FIG. 8. Diagrams for contamination through jet production and fragmentation. a,b,c,d are quarks or gluons; M are mesons (π^0,η).

$$D_c(z)=2.8\int_{w_{\min}}^{w_{\max}} D_{\pi^0/c}(w)\frac{dw}{w}+D_{\gamma/c}(z)\theta(z-\bar{z})\ , \tag{4.7}$$

where the first term on the right-hand side corresponds to the cascade process $c\to\pi^0(\eta)+\cdots\to\gamma+\cdots$ (the contribution of the η accounting for 0.4 times the π^0 contribution), while the second one represents the radiative process $c\to\gamma+\ldots$; $D_{\pi^0/c}$, $D_{\gamma/c}$ are the usual fragmentation functions.

The various integration limits and the parameter $\bar{z}$ are given by

$$z_{\min}=\frac{p_T}{p_T+\Delta E^{(\gamma)}+\Delta E^{(h)}}\ ,$$

$$w_{\min}=\mathrm{Sup}\begin{Bmatrix} z \\ 1-\dfrac{z\Delta E^{(h)}}{p_T}\end{Bmatrix}\ ,$$

$$w_{\max}=\mathrm{Inf}\begin{Bmatrix} 1 \\ z\left[1+\dfrac{\Delta E^{(\gamma)}}{p_T}\right]\end{Bmatrix}\ ,$$

$$\bar{z}=\frac{p_T}{p_T+\Delta E^{(h)}}\ .$$

Here $\Delta E^{(\gamma)}$ is the experimental upper limit for nondetection of an accompanying additional photon, as discussed in Sec. IV A. Similarly $\Delta E^{(h)}$ is defined as the experimental upper limit for nondetection of one or more accompanying hadrons; whenever this limit is exceeded, the corresponding event will be rejected.[22]

Calculations of r have been performed for the same conditions as considered in Secs. II and III. Two different values of $\langle k_T^2\rangle$ and as well of $\Delta E^{(h)}$ where assumed, while we took $\Delta E^{(\gamma)}=0.25$ GeV. The quark and gluon distribution functions were again taken from Ref. 18 with the same ingredients as before. The fragmentation functions $D_{\pi^0/q}$, $D_{\pi^0/g}$ were taken from the same authors, but were made scale invariant by assuming $Q_0^2=\infty$. Finally $D_{\gamma/q}$, $D_{\gamma/g}$ were taken from Nicolaidis[23] (one notices that $D_{\gamma/g}$ is negligibly small).

Our results are shown in Figs. 9 and 10. It appears that r does not depend very strongly either on the theoretical parameter $\langle k_T^2\rangle$ or on the experimental one $\Delta E^{(h)}$. Even when $\Delta E^{(h)}$ cannot be kept lower than 5 GeV and $\langle k_T^2\rangle$ is taken as high as 1 GeV^2, the noise/signal ratio in the range 5 GeV/$c\le p_T\le$ 10 GeV/c remains smaller than 80% for a pp collision at $\sqrt{s}=60$ GeV, and smaller than 50% for a $p\bar{p}$ collision at $\sqrt{s}=540$ GeV.

Actually, as is shown in Table I, in both cases considered most of the background is due to the first term of formula (4.3), involving the hard process $qg\to q\gamma$. On the other hand, it is interesting to notice (see Table II) that, among the two contributions to that particular term, corresponding, respectively, to the fragmentation processes $q\to\pi^0(\eta)+\cdots\to\gamma+\cdots$ and $q\to\gamma+\ldots$, the latter tends to be the larger one, especially at high p_T.

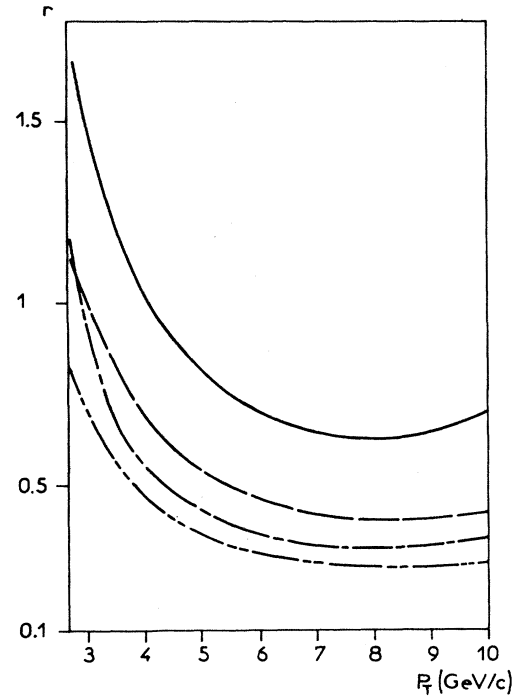

FIG. 9. Noise/signal ratio r, resulting from contamination through jet production and fragmentation, for the process $pp\to\gamma\gamma X$ at $\sqrt{s}=60$ GeV. Solid curve, $\Delta E^{(h)}=5$ GeV, $\langle k_T^2\rangle=1$ GeV; long-dashed curve, $\Delta E^{(h)}=1$ GeV, $\langle k_T^2\rangle=1$ GeV; dot-dash curve, $\Delta E^{(h)}=5$ GeV, $\langle k_T^2\rangle=0.25$ GeV; dot-dot-dash curve, $\Delta E^{(h)}=1$ GeV, $\langle k_T^2\rangle=0.25$ GeV.

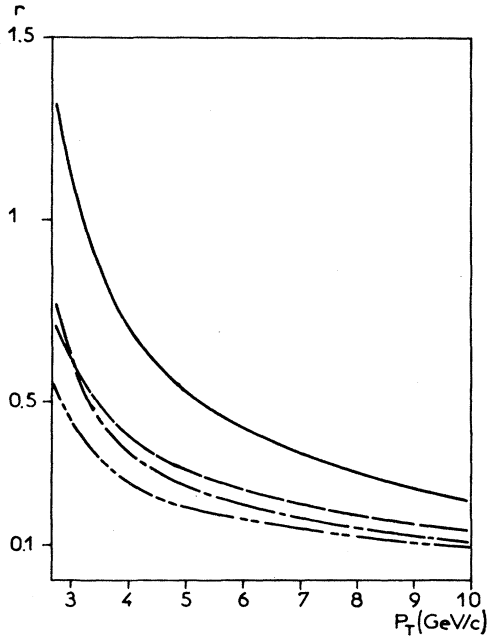

FIG. 10. Same as Fig. 9, for the process $p\bar{p}\to\gamma\gamma X$ at $\sqrt{s}=540$ GeV.

TABLE I. Ratio of the contribution of the first term in formula (4.3), involving the hard process $qg \to q\gamma$, to the total contamination. We assume $\Delta E^{(h)}=1$ GeV, $\langle k_T^2 \rangle = 1$ GeV^2.

p_T (GeV/c)	$pp \to \gamma\gamma X$ $\sqrt{s}=60$ GeV	$p\bar{p} \to \gamma\gamma X$ $\sqrt{s}=540$ GeV
3	0.88	0.85
4	0.94	0.92
5	0.96	0.95
6	0.96	0.96
7	0.97	0.97
8	0.97	0.98
9	0.97	0.98
10	0.97	0.98

TABLE II. Ratio of the contribution of the sequence of processes $qg \to q\gamma, q \to \gamma + \cdots$ (bremsstrahlung) to the total contribution of $qq \to q\gamma$ to the contamination. We assume $\Delta E^{(h)}=1$ GeV, $\langle k_T^2 \rangle = 1$ GeV^2.

p_T (GeV/c)	$pp \to \gamma\gamma X$ $\sqrt{s}=60$ GeV	$p\bar{p} \to \gamma\gamma X$ $\sqrt{s}=540$ GeV
3	0.49	0.55
4	0.60	0.69
5	0.67	0.76
6	0.72	0.83
7	0.75	0.87
8	0.78	0.90
9	0.79	0.92
10	0.80	0.93

D. Contamination due to the Brodsky-Lepage mechanism

A contribution of the Brodsky-Lepage or "fusion" mechanism,[24] i.e., direct production of particle pairs in a hard collision, to the contamination of direct-photon pair measurements is of a more hypothetical nature, since the existence of such a mechanism has not yet been proven experimentally. Therefore we are computing it separately.

The processes involved are $AB \to M\gamma X$ and $AB \to MM'X$ ($M,M' \equiv \pi^0$ or η) followed by 2γ decay of the meson(s). Some of the corresponding hard-collision diagrams are represented in Fig. 11.

It should be noticed that the hard processes $gg \to M\gamma$ as well as $gg \to \pi^0\eta$ are prohibited by conservation laws (C-parity conservation and isotopic-spin conservation, respectively). On the other hand, the amplitude of $q\bar{q} \to MM'$ happens to vanish at $\theta = 90°$.

We therefore stay with the following expression of the noise/signal ratio due to the Brodsky-Lepage mechanism:

$$r^{\mathrm{BL}} = (\bar{\sigma}^{AB\to\gamma\gamma X}_{(q\bar{q})} + \bar{\sigma}^{AB\to\gamma\gamma X}_{(gg)})^{-1} \frac{8\Delta E^{(\gamma)}}{s} \times \left[\sum_{q=u,d} (q_A \bar{q}_B + \bar{q}_A q_B) \tilde{\sigma}^{q\bar{q}\to\pi^0\gamma} + 0.4 \sum_{q=u,d,s} (q_A \bar{q}_B + \bar{q}_A q_B) \tilde{\sigma}^{q\bar{q}\to\eta\gamma} + \frac{2\Delta E^{(\gamma)}}{p_T} g_A g_B (\tilde{\sigma}^{gg\to\pi^0\pi^0} + 0.16 \tilde{\sigma}^{gg\to\eta\eta}) \right], \tag{4.8}$$

where some simplifications were introduced, using the fact that

$$\Delta E^{(\gamma)}/p_T \ll 1 .$$

We have computed

$$\tilde{\sigma}^{q\bar{q}\to\pi^0\gamma} = \frac{\pi\alpha_s\alpha e_q^{\,2}}{27 p_T^{\,2}} F_\pi , \tag{4.9}$$

where F_π is an expression related to the distribution amplitude of the component quarks of the pion, and which may be identified with the charged pion's electromagnetic form factor; we shall take $F_\pi = a/(4p_T^2)$ with $a=0.4$ GeV^2. We also obtain

$$\tilde{\sigma}^{q\bar{q}\to\eta\gamma} = \frac{\pi\alpha_s\alpha c_q e_q^{\,2}}{81 p_T^{\,2}} F_\eta , \tag{4.10}$$

where $c_q=1$ for $q \equiv u,d$; $c_q=4$ for $q \equiv s$; F_η is defined similarly to F_π; by analogy ("nonet symmetry") we take $F_\eta = F_\pi$.

As for the calculation of $\tilde{\sigma}_{gg\to MM}$, it involves a large number of diagrams, which can be divided into two groups. Those whose analogs (replacing the initial photons by gluons) were considered by Brodsky and Lepage[24] in their calculation of $\gamma\gamma \to \pi^0\pi^0$ [one such typical diagram is shown in Fig. 11(d)]; and those who have no analogs in $\gamma\gamma$ collisions [as shown, for instance, in Fig. 11(e)]. It appears that, at $\theta = 90°$, the total amplitude of the second group of diagrams amounts to zero, so that one gets the relation (taking account of a charge and color factor)

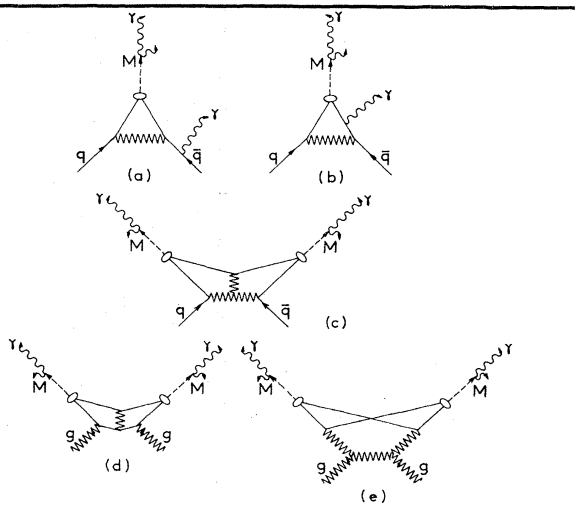

FIG. 11. Various typical diagrams for contamination through the Brodsky-Lepage (fusion) effect. M are mesons (π^0, η).

$$\tilde{\sigma}^{gg\to\pi^0\pi^0}=\frac{9}{50}\frac{\alpha_s^{\,2}}{\alpha^2}\tilde{\sigma}^{\gamma\gamma\to\pi^0\pi^0}\ . \tag{4.11}$$

Using nonet symmetry the same expression is obtained for $\tilde{\sigma}^{gg\to\eta\eta}$. $\tilde{\sigma}^{\gamma\gamma\to\pi^0\pi^0}$ is taken from Ref. 24 as

$$\tilde{\sigma}^{\gamma\gamma\to\pi^0\pi^0}=\frac{25}{162}\frac{\pi\alpha^2}{p_T^{\,2}}F_\pi^{\,2}g^2(\pi/2;\phi_\pi)\ ,$$

where one assumes again $F_\pi=0.1\ \text{GeV}/p_T^{\,2}$.

As for $g^2(\pi/2;\phi_\pi)$, its numerical value is given in Ref. 24 for three different options proposed for the distribution amplitude ϕ_π. Choosing the option[25] $\phi_\pi\sim[x(1-x)]^{1/4}$, one gets $g^2(\pi/2;\phi_\pi)\simeq\frac{1}{3}$.

Using the quark and gluon distribution functions from Ref. 18 as before, one gets the values of r^{BL} given in Table III. It is seen that they are rather small and go rapidly to zero with increasing p_T.

TABLE III. Noise/signal ratio due to the Brodsky-Lepage (fusion) effect.

p_T (GeV/c)	$pp\to\gamma\gamma X$ $\sqrt{s}=60$ GeV	$p\bar{p}\to\gamma\gamma X$ $\sqrt{s}=540$ GeV
3	5.0%	4.1%
4	1.9%	1.1%
5	0.9%	0.5%
6	0.5%	0.3%
7	0.3%	0.2%
8	0.2%	0.1%
9	0.1%	0.1%
10	0.1%	0.1%

V. CONCLUSION

Direct-photon pair production has been shown to have a high potential for new checks of quantum chromodynamics and perhaps a discovery of new particles and structures. While the yields to be expected for this process in high-energy hadron collisions are about the same as for lepton pair production (Drell-Yan process), its physical interest appears to be even greater.

The main difficulty (and deterrent for experimentalists) is that measurements of this process are expected to involve a huge background due to various sources of indirect photons. In this paper we have shown that, under specific conditions, that background can be reduced to reasonable proportions. The conditions here envisaged are the following:

(a) Use of colliding beams of high-energy hadrons.

(b) Detection of outgoing photons close to 90° (in order to have a large angular range available for vetoing accompanying hadrons or additional photons).

(c) Measurement of two photons with equal and opposite momenta, unaccompanied by any other particles (as far as this can be experimentally checked).

To a large extent, actually, those conditions were realized in the recent ISR experiment mentioned.[5] As our calculations show, one should be able to obtain a still better background suppression in a similar experiment performed at higher energy, e.g., with the CERN collider.

Some 15 years ago, it was proposed to study $\gamma\gamma$ collisions;[26] in spite of considerable experimental difficulties, $\gamma\gamma$ collision physics has now become an important and fascinating area of investigation, providing us with a large amount of new physical information. The reverse process, i.e., $\gamma\gamma$ production as considered here, appears fit to become a complementary source of information. We have no doubt that in some future it will give rise, as well, to an interesting field of research in high-energy physics.

[1]S. D. Drell and T.-M. Yan, Phys. Rev. Lett. 25, 1523 (1970); Ann. Phys. (N.Y.) 66, 578 (1971).

[2]J. J. Aubert *et al.*, Phys. Rev. Lett. 33, 1404 (1974).

[3]S. W. Herb *et al.*, Phys. Rev. Lett. 39, 252 (1977).

[4]C. N. Yang, Phys. Rev. 77, 242 (1950).

[5]C. Kourkoumelis *et al.*, Z. Phys. C 16, 101 (1982).

[6]S. M. Berman, J. D. Bjorken, and J. B. Kogut, Phys. Rev. D 4, 3388 (1971).

[7]K. S. Soh, P. Y. Pac, H. W. Lee, and J. B. Choi, Phys. Rev. D 18, 751 (1978).

[8]M. Krawczyk and W. Ochs, Phys. Lett. 79B, 119 (1978).

[9]S. Hemmi, Prog. Theor. Phys. 63, 1073 (1980).

[10]B. L. Combridge, Nucl. Phys. B174, 243 (1980).

[11]C. Carimalo, M. Crozon, P. Kessler, and J. Parisi, Phys. Lett. 98B, 105 (1981).

[12]A. P. Contogouris, L. Marleau, and B. Pire, Phys. Rev. D 25, 2459 (1982).

[13]R. D. Field, in *Proceedings of the Fifth International Workshop on Photon-Photon Collisions, Aachen,* edited by Ch. Berger (Springer, Berlin, 1983), p. 1.

[14]See, for instance, K. Kajantie, Acta Phys. Austriaca Suppl. 21, 663 (1979); our formula (2.1) can be derived from Eq. (2.6) there by means of a trivial change of variables.

[15]Derived from the calculation of the inverse process by R. N. Cahn and J. F. Gunion, Phys. Rev. D 20, 2253 (1979), which was itself based on an old QED calculation by B. De Tollis, Nuovo Cimento 32, 757 (1964); 35, 1182 (1965).

[16]Actually the selection rules for coupling to two gluons are somewhat more restrictive than for coupling to two photons; i.e., only flavor-singlet states can be coupled to gg.

[17]M. B. Einhorn and S. D. Ellis, Phys. Rev. Lett. 24, 1190 (1975).

[18]R. Baier, J. Engels, and B. Petersson, Z. Phys. C 2, 265 (1979).

[19]In the experiment described in Ref. 5, for instance, the following ratios of particle yields were found (in a p_T range extending from 2 to 9 GeV): $\eta/\pi^0=0.55\pm0.07$, $\omega/\pi^0=0.87\pm0.17$, $\eta'/\pi^0=0.90\pm0.25$.

[20]J. F. Gunion and B. Petersson, Phys. Rev. D 22, 629 (1980); see, in particular, Eqs. (A1)—(A8) of the Appendix.

[21]B. L. Combridge, J. Kripfganz, and J. Ranft, Phys. Lett. 70B, 234 (1977).

[22]By "accompanying hadrons" we mean of course that those

hadrons belong to the same jet as the photon measured. In other words, the measurement to be performed should involve an angular range of 20—30° around either photon, where hadrons of total energy larger than $\Delta E^{(h)}$ would be vetoed.

[23]A. Nicolaidis, Nucl. Phys. B163, 156 (1980).

[24]S. J. Brodsky and G. P. Lepage, Phys. Rev. D 24, 1808 (1981).

[25]This option is the only one, among the three proposed, which makes both ways of normalizing ϕ_π [see Eqs. (4) and (5) of Ref. 24] compatible with each other and with a reasonable value of α_s. Let us notice here that a very different choice of ϕ_π, made by V. I. Chernyak and A. R. Zhitnitsky [Nucl. Phys. B22, 382 (1983)] on the basis of QCD sum rules, leads to practically the same value of $\tilde{\sigma}^{\gamma\gamma\to\pi^0\pi^0}$ as that used here.

[26]N. Arteaga-Romero, A. Jaccarini, and P. Kessler, C. R. Acad. Sci. Ser. 269B, 153 (1969); 269B, 1129 (1969); V. E. Balakin, V. M. Budnev, and I. F. Ginzburg, Pis'ma Zh. Eksp. Teor. Fiz. 11, 559 (1970) [JETP Lett. 11, 388 (1970)]; S. J. Brodsky, T. Kinoshita, and H. Terazawa, Phys. Rev. Lett. 25, 972 (1970).